International Journal of Nanomedicine

Dovepress
open access to scientific and medical research

Open Access Full Text Article

ORIGINAL RESEARCH

A TA/Cu^{2+} Nanoparticle Enhanced Carboxymethyl Chitosan-Based Hydrogel Dressing with Antioxidant Properties and Promoting Wound Healing

Yongjun Huang[1,*], Yong Chen[2,*], Guoyun Cheng[1,*], Wenqiang Li[3], Hongan Zhang[1,4], Chaoqun Yu[1], Jia Fang[1], Jieyi Zuo[1], Ying Li[1], Lei Xu[1], Dawei Sun[1]

[1]Department of Orthopedics, Guangdong Second Provincial General Hospital, Guangzhou, 510317, People's Republic of China; [2]Department of Orthopedics, The Sixth Affiliated Hospital of Guangzhou Medical University, Qingyuan, People's Hospital, Qingyuan, 511518, People's Republic of China; [3]Engineering Technology Research Center for Sports Assistive Devices of Guangdong, Guangzhou Sport University, Guangzhou, 510500, People's Republic of China; [4]The Second Clinical School of Medicine, Southern Medical University, Guangzhou, 510260, People's Republic of China

*These authors contributed equally to this work

Correspondence: Lei Xu; Dawei Sun, Department of Orthopedics, Guangdong Second Provincial General Hospital, 11th Floor, Building 3, No. 466, Xingang Middle Road, Guangzhou, Guangdong Province, 510317, People's Republic of China, Email orthoxl@163.com; sundw@gd2h.org.cn

Background: As the first line of immune defense and the largest organ of body, skin is vulnerable to damage caused by surgery, burns, collisions and other factors. Wound healing in the skin is a long and complex physiological process that is influenced by a number of different factors. Proper wound care can greatly improve the speed of wound healing and reduce the generation of scars. However, traditional wound dressings (bandages, gauze, etc.) often used in clinical practice have a single function, lack of active ingredients and are limited in use. Hydrogels with three-dimensional network structure are a potential biomedical material because of their physical and chemical environment similar to extracellular matrix. In particular, hydrogel dressings with low price, good biocompatibility, degradability, antibacterial and angiogenic activity are favored by the public.

Methods: Here, a carboxymethyl chitosan-based hydrogel dressing (CMCS-TA/Cu^{2+}) reinforced by copper ion crosslinked tannic acid (TA/Cu^{2+}) nanoparticles was developed. This study investigated the physical and chemical characteristics, cytotoxicity, and angiogenesis of TA/Cu^{2+} nanoparticles and CMCS-TA/Cu^{2+} hydrogels. Furthermore, a full-thickness skin defect wound model was employed to assess the in vivo wound healing capacity of hydrogel dressings.

Results: The introduction of TA/Cu^{2+} nanoparticles not only could increase the mechanical properties of the hydrogel but also continuously releases copper ions to promote cell migration (the cell migration could reach 92% at 48 h) and tubule formation, remove free radicals and promote wound healing (repair rate could reach 90% at 9 days).

Conclusion: Experiments have proved that CMCS-TA/Cu^{2+} hydrogel has good cytocompatibility, antioxidant and wound healing ability, providing an advantageous solution for skin repair.

Keywords: TA/Cu^{2+} nanoparticles, carboxymethyl chitosan, wound dressing, antioxidant activity

Introduction

As the first line of defense of body, the skin protects us from physical, chemical and biological stimuli from the external environment.[1–3] However, there are significant challenges in clinical practice when it comes to skin injuries caused by bacterial infections, external stimuli or autologous organ necrosis.[4–6] Due to the improper management of skin wounds, skin disease has become one of the leading causes of morbidity and mortality worldwide.[7–9] To heal, the skin must undergo overlapping phases of hemostasis, inflammation, proliferation and remodeling, and each stage is crucial to the healing process.[10–12] Conventional therapeutic approaches like the use of gauze serve to safeguard the wound against contamination. However, these dressings possess a sole purpose of offering physical protection, thus failing to create an optimal biological milieu conducive to wound healing or facilitate the release of active agents that stimulate the process.[5,13–15] In the field of skin

Received: 20 October 2023
Accepted: 28 December 2023
Published: 10 January 2024

Graphical Abstract

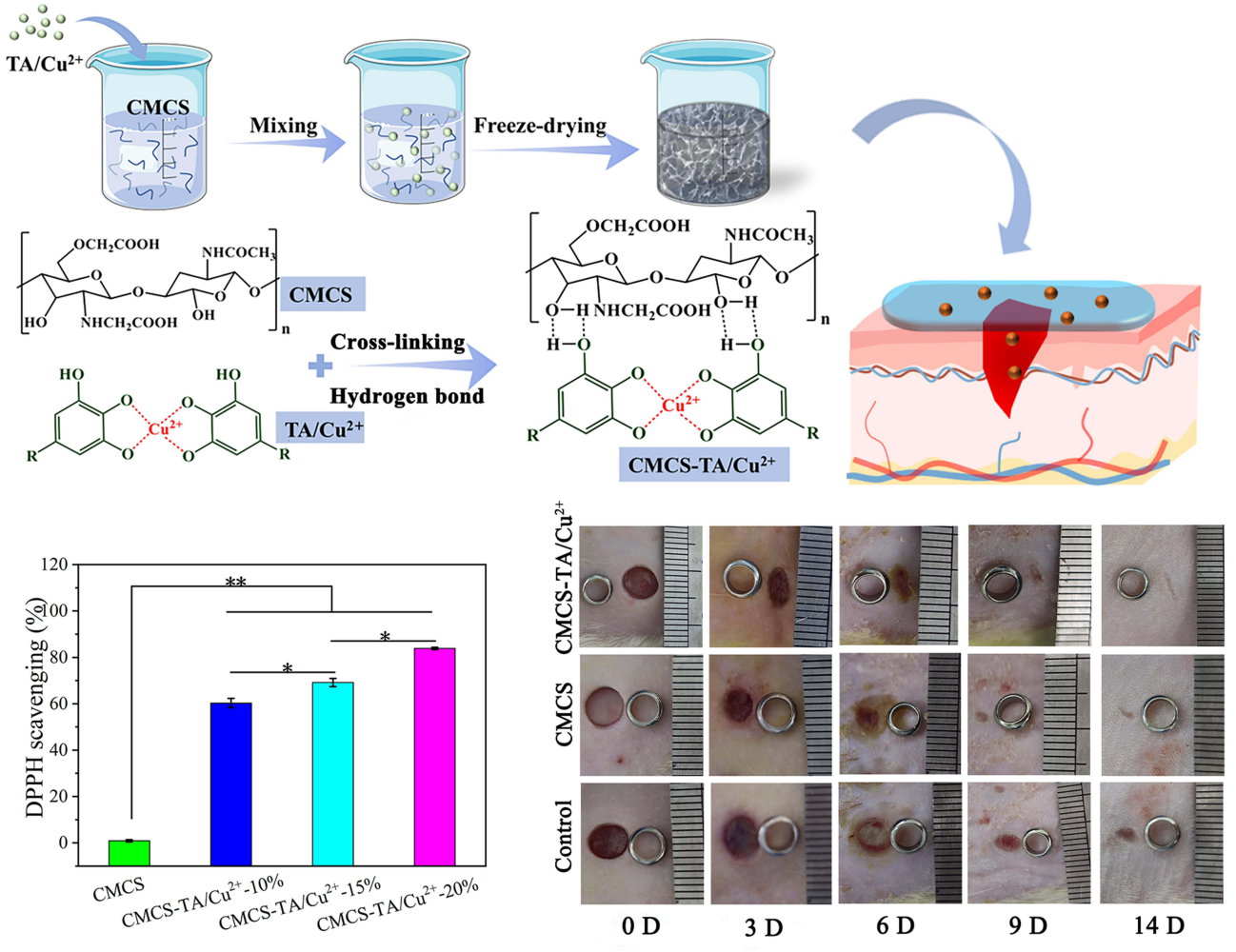

repair, a number of synthetic materials have been developed for wound healing, such as the preparation of electrostatically spun fiber membranes loaded with highly active adipose stem cells[16] and the electrostatically spun preparation of chitosan/polyvinyl alcohol fibers.[17] However, the poor structural similarity of these membrane-based dressings to the natural extracellular matrix (ECM) makes it difficult for cells to adhere and proliferate, slows wound healing, has poor hygroscopicity that can easily lead to the accumulation of submembrane exudates, and lacks antimicrobial properties, which can easily induce or aggravate infections.

Hydrogel has been developed to address the problems of skin repair.[18–20] Hydrogels are able to form a physical barrier and create a moist environment to promote wound repair due to their similar structure to the ECM.[11,20–24] In particular, natural polymer-based hydrogels, such as carboxymethyl chitosan (CMCS) hydrogels, have excellent biocompatibility and bioactivity, which can promote cell proliferation and tissue remodeling and effectively facilitate wound healing.[25–28] Due to its similarity to human tissue chemistry, carboxymethyl chitosan hydrogel provides a suitable mechanical microenvironment, while reducing the risk of scarring and improving wound aesthetics.[14,29,30] Yue et al developed a CMCS-based hydrogel dressing loaded with active peptides that can effectively promote the healing of diabetic wounds.[31] However, CMCS hydrogels have inherently poor antimicrobial properties and lack long-lasting active ingredients (active ingredients such as peptides are prone to inactivation) to promote tissue repair, which limits their use in skin repair. Tannic acid (TA) is a naturally occurring organic compound found in plants. It plays a protective role in plants and can improve the antibacterial, insect and antioxidant capacity of plants. TA is also

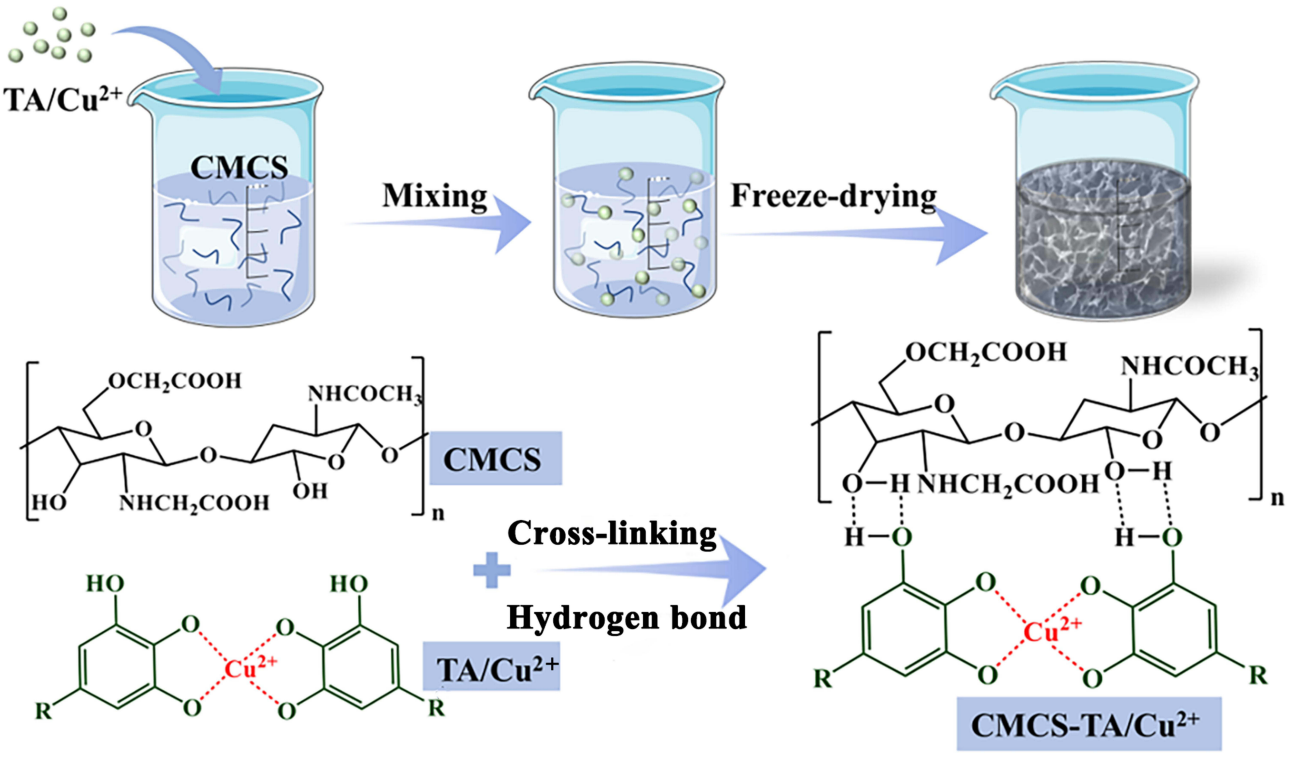

Figure 1 Preparation process diagram of the CMCS-TA/Cu^{2+} hydrogel (The red text mark indicates the formation of a coordination bond between Cu^{2+} and TA in the TA/Cu^{2+} nanoparticle).

a natural polyphenol compound that inhibits oxidative stress and the production of free radicals to protect cells from damage, and it also has certain anti-inflammatory effects, which can reduce the inflammatory response around the wound and promote wound repair.[32] In addition, TA constricts blood vessels, reduces bleeding from wounds, and helps the wound form blood clots and scar tissue. Copper (Cu) is a trace element that plays an important role in wound repair. Copper ions (Cu^{2+}) are involved in the synthesis of collagen and promote wound healing. Cu^{2+} also has antibacterial effects that can help prevent wound infections, keep wounds clean, and speed up the healing process.[33–35] Excessive Cu^{2+} at the wound site often causes a toxic reaction that worsens the injury. Huang et al developed a cu-ion cross-linked epigallocatechin gallate hydrogel, which has good angiogenic and antioxidant activity, and can effectively promote wound healing at the burn site.[36] In order to balance the biocompatibility and angiogenic activity of material, copper ion crosslinked tannic acid (TA/Cu^{2+}) nanoparticles were synthesized, a composite with excellent antioxygenic and antimicrobial capacities.

As shown in Figure 1, a hydrogel dressing (CMCS-TA/Cu^{2+}) made of carboxymethyl chitosan and copper ion cross-linked tannic acid nanoparticles was created. TA/Cu^{2+} nanoparticles with excellent antioxygenic and pro-repairing abilities were formed by chelation of copper ions with tannic acid. Then TA/Cu^{2+} nanoparticles were combined with carboxymethyl chitosan solution, and the CMCS-TA/Cu^{2+} hydrogel dressing was prepared by lyophilization. The mechanical properties of the hydrogels were significantly improved by the hydrogen bonding between the nanoparticles and the CMCS network. The composite CMCS-TA/Cu^{2+} hydrogel was found to have excellent antioxidant properties and the ability to facilitate skin repair. Additionally, it exhibits excellent biocompatibility. Consequently, it holds great practical application value as a biomedical material.

Experimental and Methods

Materials

Tannic acid (TA, AR) and carboxymethyl chitosan (CMCS, 190,000–310,000Da) were supplied by Shanghai Macklin Biochemical Technology Co. Ltd. Poly(ethylene oxide)-poly(propylene oxide)-poly(ethylene oxide) triblock copolymer

(F127) and Copper sulfate pentahydrate ($CuSO_4 \cdot 5H_2O$, AR) were provided by Aladdin Reagent (Shanghai) Co. Ltd. The remaining chemical reagents were of analytical grade and used without further processing.

Manufacture of CMCS-TA/Cu^{2+} Hydrogel Dressing

Previous papers state that the sol–gel approach was used to synthesize the TA/Cu^{2+} nanoparticles.[37,38] F127 (0.4 g) was first dissolved in 96 mL of water and 16 mL of ethanol. Next, for 1 hr, 0.8 mL ammonia solution (28 wt%) was added and swirled. Then, tannic acid (0.4 g) and formaldehyde solution (0.76 mL, 37 wt%) was added, and the mixture was agitated for a further 24 h. After the solution had been stirring for a full day, 4 mL of 0.5 wt% $CuSO_4 \cdot 5H_2O$ solution was added and swirled once again. Subsequently, the mixture was moved to a 150 mL high-pressure reactor and hydrothermally treated for 24 h at 100°C. Centrifugation, washing, and freeze-drying were used to gather the resultant sample. The morphology of the TA/Cu^{2+} nanoparticles was studied with the transmission electron microscope (TEM, Japan, Philips TECNAI 10). The size of nanoparticles was measured in TEM images using Image J software.

A certain mass of CMCS was weighed and fully dissolved in deionized water (2 wt%). TA/Cu^{2+} nanoparticles were added to the above CMCS solution, mixed well, poured into the mold, and freeze-dried. According to the mass ratio of TA/Cu^{2+} nanoparticles to CMCS in the hydrogel precursor solution is 10%, 15%, and 20%, the prepared hydrogel is named CMCS-TA/Cu^{2+}-10%, CMCS-TA/Cu^{2+}-15%, and CMCS-TA/Cu^{2+}-20%, in order.

Swelling Properties and Microstructure

The swelling behavior of the hydrogels was studied by gravimetric analysis; the hydrogels were freeze-dried and weighed (W_d) and infiltrated in water; when the swelling equilibrated, the surface water was drained by filter paper and the mass (W_s) was recorded. The swelling ratio rate was determined using the provided equation (1)[39]

$$\text{Swelling ratio}(\%) = \frac{W_s - W_d}{W_d} \times 100\% \quad (1)$$

Porosity was determined by the liquid replacement method, using ethanol as the replacement liquid; in short, a certain volume of lyophilized hydrogel was immersed in ethanol, just enough to saturate the lyophilized hydrogel. Material was removed after 24 hr and weighed (W_2). The porosity (P) was determined based on the following equation (2)[40]

$$P = \frac{W_2 - W_1}{\rho V_1} \quad (2)$$

Where W_1 and W_2 represent the mass of the hydrogel prior to and following immersion, respectively. V_1 represents the alcohol volume prior to immersion, and ρ represents the density of the alcohol, which is a constant.

The freeze-dried CMCS-TA/Cu^{2+} hydrogel was sprayed with gold and observed under the scanning electron microscope (SEM, SU9000) to determine the composites' microscopic morphology.

FTIR and XRD Analysis

Fourier Transform Infrared Spectrometer (FTIR) spectra were obtained using an FTIR spectrometer (MAGNA 560, Nicolet, USA) at 25°C with a wave number of 500–4000 cm^{-1}.

The X-Ray Diffractometer (XRD, Shimadzu XRD6000) patterns of CMCS, TA/Cu^{2+}, and CMCS-TA/Cu^{2+} were measured at a test voltage of 40 kV, at an angle of 2θ from 5° to 60° and at a rate of 0.02 °/min.

DPPH Antioxidant Test

The antioxidant property of the hydrogel was determined using an in vitro DPPH free radical scavenging assay. Three milligrams of lyophilized hydrogel material was added to 4 mL of 100 μM DPPH methanol solution and incubated for a period of time protected from light. The solution's absorbance (A_c) at 517 nm was calculated by UV spectrophotometer and the radical scavenging rate was calculated using the absorbance (A_s) of the DPPH solution without the added material as a blank control, following equation[41] (3).

$$\text{DPPH scavenging (\%)} = \frac{A_s - A_c}{A_c} \times 100\% \quad (3)$$

In vitro Release of Cu^{2+}

To comprehend the in vitro discharge of copper ions out of the material, a given mass of lyophilized hydrogel was submerged in 0.1 M phosphate buffered saline (PBS) at 37°C for a limited time interval (1, 3, 5, 7, 10, 14 days), and the ion discharge solution was collected by ICP inductively coupled plasma spectrometry for measurement of the ion concentration and calculation of the cumulative discharge concentration of copper ions.[42]

Cytocompatibility and Angiogenesis in vitro

The cytocompatibility of the hydrogel was assessed through testing on Human Umbilical Vein Endothelial Cells (HUVECs, purchased from Guangzhou Anbang Biotechnology Co., LTD). Shortly after being shaped into cylinders with a 7 mm diameter and 1 mm thickness, the hydrogels were lyophilized. After being submerged in 75% alcohol for 30 min, the samples were exposed to UV light for 2 hr, and three times in PBS for 5 min each, before being seeded with cells. Following this, 48-well plates containing DMEM medium (Gibco) were filled with aseptic samples, and the next day, HUVECs (1.5×10^4 cells/mL) were seeded onto the hydrogels. These cells were then cultured for 5 days at 37°C in a 5% CO_2 incubator. Each hydrogel sample was subjected to four replications. The cytotoxicity of HUVECs grown on the test materials for 1, 3, and 5 days was evaluated with the Cell Counting Kit-8 (CCK-8; Nanjing Jiancheng Technology Co., Ltd., Nanjing, China). The optical density (OD) at 450 nm is used to measure the result of cell proliferation. Following repeated labeling with acridine orange/ethidium bromide (AO/EB) for live/dead cell differentiation, examination of the cells was performed under an inverted fluorescent microscope. The morphology and cytoskeleton structure of the HUVECs were analyzed using CLSM, with the HUVECs being cultivated on the samples. Three days of cell culture were followed by a brief fixation in 4% paraformaldehyde, permeabilization in 0.1% Triton X-100, blocking in bovine serum albumin, and fluorescence staining in the dark with rhodamine-conjugated phalloidin for F-actin filament and 4',6-diamidino-2-phenylindole (DAPI, Life) for nucleus.[43]

HUVECs were injected into 24-well plates (3×10^5 cells/well) and cultured for a day in a cell incubator. Following the scratching procedure, a 200 μm sterile plastic pipette was utilized, and materials from various components as well as serum-free culture media were put to the orifice plate for co-culture (n=4). Pictures were captured at 0, 24, and 48 hr in the experiment. Cell migration rate (MR) is calculated by equation (4).

$$\text{MR} = \frac{L_0 - L_t}{L_0} \times 100\% \quad (4)$$

The L_t was the width of the scratch following the cell culture, and L_0 was its original width.

The influence of hydrogel material on angiogenesis was examined using the endovascular formation method. Prior to incubating at 37°C for 30 min, the 96-well plate was equally coated with matrix glue (10 μL/well). The HUVECs were then introduced (5000 cells/well) and cultured there for 1–2 hr. Fresh, serum-free media containing various components were added after the supernatant was discarded for continued growth, and after 12 to 24 hr, tubules began to form.

In vivo Wound Healing Experiments

All animal treatments were authorized by Southern Medical University's Animal Ethics Committee and carried out in compliance with the university's Guidelines for Care and Use of Laboratory Animals (Ethical certificate number: SYXK(Yue)2023–0417). Twenty-four male Sprague-Dawley rats (300–350 g) provided by the Guangdong Provincial Laboratory Animal Centre were used to demonstrate the wound-healing performance using hydrogel. The rats were anaesthetized with sodium pentobarbital (30 mg/kg) prior to receiving three circular wounds (5 mm diameter) on their backs. These wounds were produced through the use of a 5 mm puncture perforator. One of the wounds was left unattended and served as a blank control group, while the remaining two wounds were treated with hydrogel dressings. The hydrogel dressings comprised CMCS for one wound (CMCS group) and CMCS-TA/Cu^{2+}-20% hydrogels (CMCS-TA/Cu^{2+} group) for the other wound (n=4). Vaseline gauze and elastic bandage were used to fix the hydrogel at the

wound site. The wound closure process was captured for each sample with a digital camera at 0, 3, 6, 9, and 14 days, and subsequently, the healing rate of the wound was computed. Six rats were euthanized at random on days 7 and 14 after wound healing. The wound sites, as well as the surrounding tissues, were obtained and treated by fixation using a 10% paraformaldehyde solution. Afterward, the samples were embedded in paraffin. To analyze tissue morphology, regeneration, and collagen deposition, we employed hematoxylin and eosin (H&E) and Masson trichrome staining on the sections. H&E staining is commonly used for visualizing cellular structures, while Masson trichrome staining is used to highlight collagen fibers in tissues. This staining technique allows for the evaluation and visualization of tissue healing and collagen deposition in the examined samples.[44]

Statistical Analysis

All data are presented in averages. Paired *t*-test and one-way ANOVA with Fisher's post hoc test for multiple comparisons were performed on the normalized data using SPSS software.[45] Significance was accepted at $*p<0.05$, statistically higher significant at $**p<0.01$, and most significant at $***p<0.001$.

Discussion and Results

Structural Analysis of the TA/Cu^{2+} Nanoparticles and Hydrogels

In the alkaline environment, tannic acid formed tannic acid polymerization network through acetal reaction and oxidation self-polymerization, and then crosslinked with copper ions to prepare TA/Cu^{2+} nanoparticles. The TA/Cu^{2+} nanoparticles are regular spheres whose diameters are concentrated in 70–90 nm (Figure 2A and B). Moreover, it can be seen from Figure 2C that the FTIR curves of TA and TA/Cu^{2+} had absorption peaks at 3450 cm^{-1}, which are the stretching vibration peaks generated by -OH in the aromatic ring.[38] However, the absorption peak at 3450 cm^{-1} of the TA/Cu^{2+} curve was wider and stronger than TA, which was due to the complexation of Cu^{2+} with the phenol hydroxyl group on TA. In addition, in the TA infrared spectrum curve, an absorption peak appeared at the position of 1540 cm^{-1}, which was the asymmetric stretching vibration characteristic peak of the carboxylic acid functional group in tannic acid. In the TA/Cu^{2+} infrared spectrum curve, the absorption peak at the position of 1540 cm^{-1} disappeared, and the absorption peak of

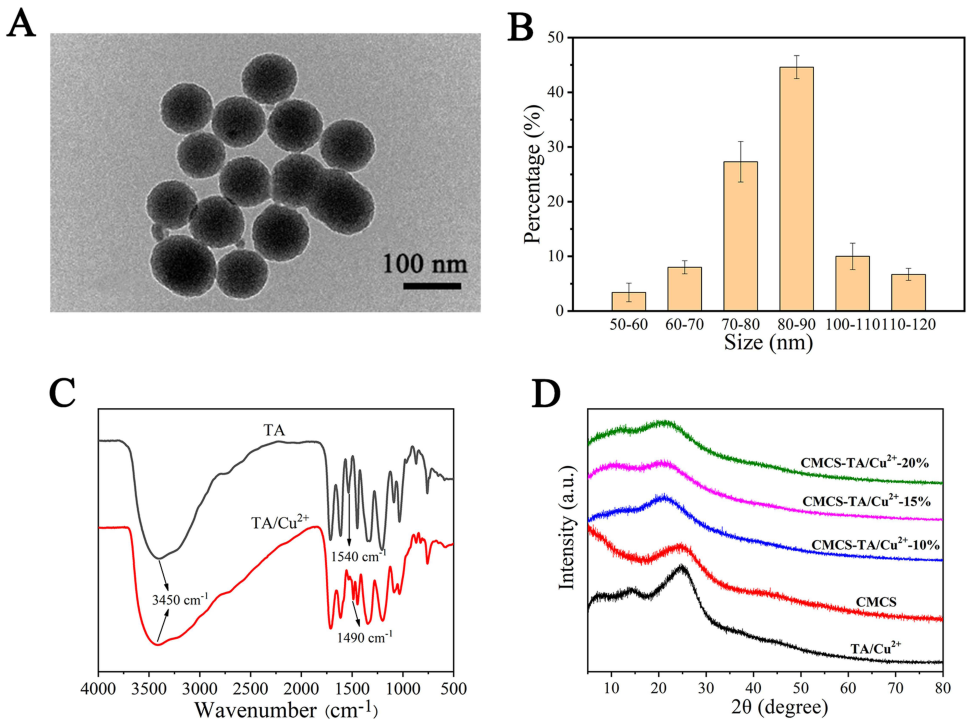

Figure 2 (**A**) TEM images of TA/Cu^{2+}nanoparticles, (**B**) Particle size distribution of TA/Cu^{2+} hydrogels. (**C**) FTIR spectra of TA and TA/Cu^{2+} hydrogels. (**D**) XRD profiles of various hydrogels.

1490 cm^{-1} appeared, which was also due to the chelation of copper ions and tannic acid, resulting in the infrared characteristic peak of carboxylic acid groups in tannic acid.[38]

To study the dispersion of TA/Cu^{2+} nanoparticles in CMCS, the obtained materials were analyzed with XRD spectra, as shown in Figure 2D, the XRD spectra of CMCS and TA/Cu^{2+} nanoparticles show a steamed bun-shaped peak, indicating that both are amorphous structures. With the cross-linking of CMCS and TA/Cu^{2+} nanoparticles, the XRD patterns of CMCS-TA/Cu^{2+} hydrogel showed a decrease in the intensity of the characteristic peaks at 2θ=20–30° compared to that of TA/Cu^{2+} nanoparticles, and the peak positions were shifted, which could be attributed to the cross-linking of TA/Cu^{2+} nanoparticles, with CMCS further reducing the number of exposed phenolic groups in TA/Cu^{2+} nanoparticles. The XRD spectra of the characteristic peak intensities between CMCS-TA/Cu^{2+} hydrogels did not show any significant difference, indicating that TA/Cu^{2+} nanoparticles entered the gel interlayer and may be uniformly dispersed in the gel system at the micron scale.

Swelling Characteristics and Morphological Analysis

The swelling behavior of the hydrogels was investigated by gravimetric analysis. The results obtained are shown in Figure 3A, which shows that the swelling rate of CMCS hydrogels reached 747%, indicating that the CMCS hydrogels have excellent water absorption and storage capacity. The swelling rates of CMCS-TA/Cu^{2+} hydrogels at different ratios (10%, 15%, 20%) were 1552%, 1173%, and 838%, respectively. The swelling rate of CMCS-TA/Cu^{2+} hydrogel showed a decreasing trend with increasing dosage of the TA/Cu^{2+} nanoparticles. In the swelling process, water molecules continue to enter the hydrogel, the volume of CMCS hydrogel is expanded, and the physical entanglement and hydrogen bond in the hydrogel is weakened, resulting in the collapse of part of the hydrogel network and no longer absorb water. With the introduction of TA/Cu^{2+} nanoparticles, the physical and chemical double cross-linked CMCS-TA/Cu^{2+} hydrogel enhances its rigidity (chemical bond is not easy to break), and the hydrogel network is not easy to collapse during water absorption. With the increase of TA/Cu^{2+} nanoparticles, the chemical crosslinking density increases, the hydrogel rigidity increases, and the absorption performance

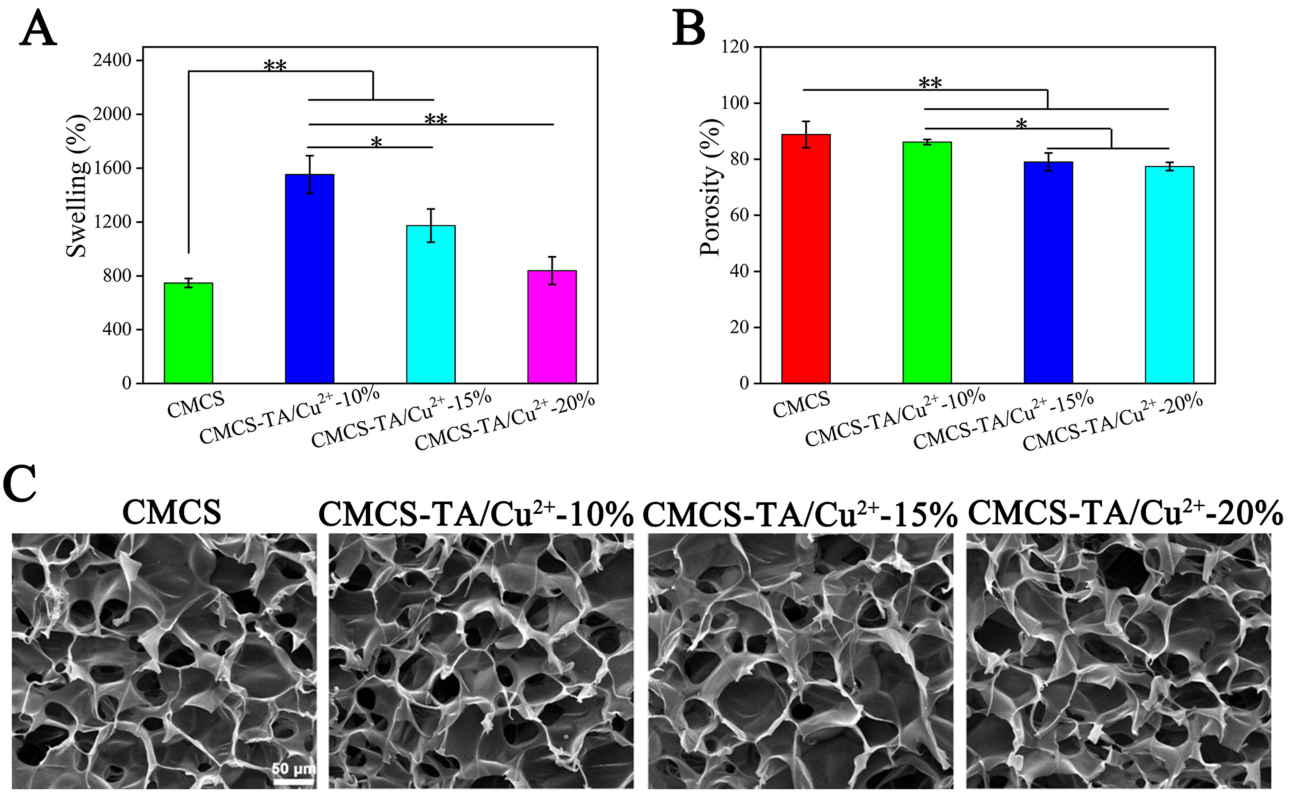

Figure 3 (**A**) Swelling rate. (**B**) Porosity and (**C**) SEM images of various hydrogels. A one-way ANOVA was used to determine statistical significance: *$p < 0.05$, **$p < 0.01$.

decreases. Therefore, the swelling rate of CMCS-TA/Cu^{2+}-10% hydrogel is higher than that of CMCS and other components of hydrogel.

The alcohol displacement method was used to determine the materials' porosity. Equation (2) is used to calculate the porosity, and the resulting data is depicted in Figure 3B. The porosity of CMCS was found to be 84–93% of the total volume, whereas the porosity of the TA/Cu^{2+} doped CMCS-TA/Cu^{2+} hydrogel was 75%–87%. The samples' decrease in porosity was not significant compared to the CMCS hydrogel, and it was due to the interaction of CMCS with TA/Cu^{2+} nanoparticles. The solvent used was ethanol, which did not swell the freeze-dried CMCS hydrogels. The porosity of the hydrogel, whereby pore size plays a significant role, determines its capability to absorb wound exudate or facilitate the transport of nutrients and oxygen. Efficient fluid absorption assists in controlling infection at the wound site.

The hydrogels were freeze-dried and examined using a SEM to further understand the microscopic morphology of the materials. The results are shown in Figure 3C. As can be seen, the pores of the CMCS-TA/Cu^{2+} hydrogel were interconnected. With the addition of TA/Cu^{2+} nanoparticles, the pore size of the hydrogel changed slightly, which was consistent with the trend of the porosity data above. The phenomenon is caused by the hydrogen bond cross-linking between CMCS and TA/Cu^{2+} nanoparticles, and the degree of cross-linking of the hydrogel gradually increases, and thus the pore size becomes smaller.

DPPH Antioxidant Analysis

The hydrogel's antioxidant capacity was measured by determining its ability to scavenge the stable free radical DPPH, and the results are shown in Figure 4. The intensity of the DPPH absorption peak at 516 nm of CMCS was almost indistinguishable from that of the blank group, indicating that the CMCS had almost no antioxidant property, and the intensity of the DPPH absorption peak at 516 nm was significantly reduced with the increase of the TA/Cu^{2+} nanoparticles content, and the better the free radical scavenging effect was. Within 5 min, the free radical scavenging rate reached 60% in the CMCS-TA/Cu^{2+}-10% group and 83% in the CMCS-TA/Cu^{2+}-20% material group. This hydrogel dressing with good antioxidant properties can remove free radicals and reduce the effect of oxidative stress on the wound, while also reducing the inflammatory response, helping to reduce the degree of inflammation around the wound and promoting tissue repair and regeneration.[46]

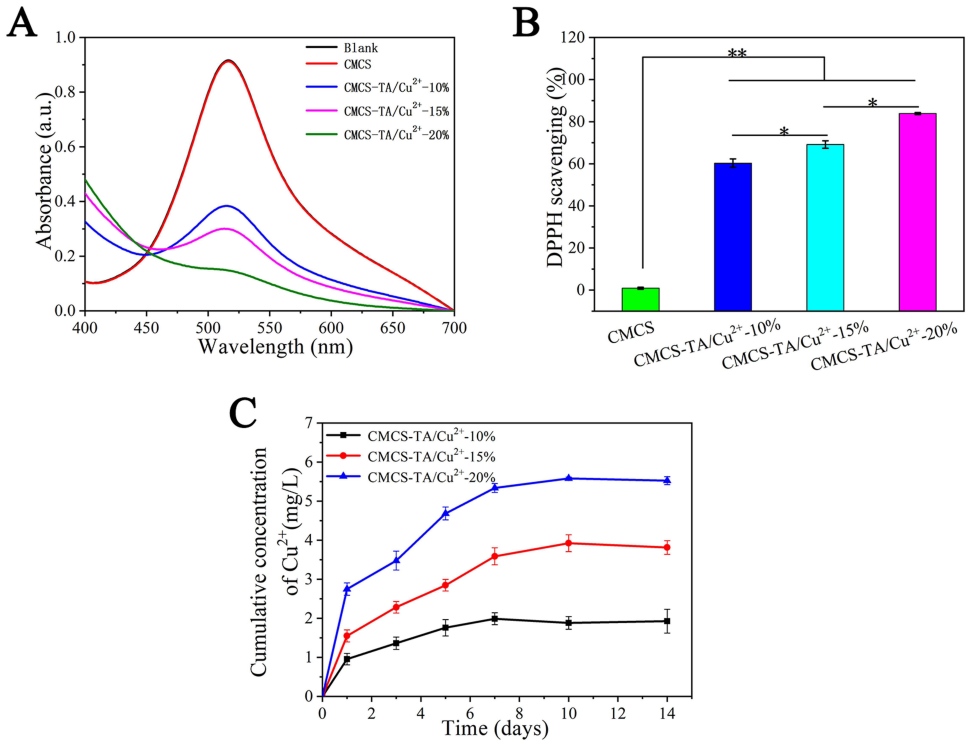

Figure 4 (**A**) UV-vis spectra of different components. (**B**) DPPH quenching efficiency. (**C**) Release rate of Cu^{2+} from CMCS-TA/Cu^{2+} hydrogels for 14 days in vitro. A one-way ANOVA was used to determine statistical significance: *$p < 0.05$, **$p < 0.01$.

Analysis of the Release of Cu^{2}+ in vitro

The copper ion release curves of hydrogel materials with different TA/Cu^{2+} nanoparticles contents in 14 days are shown in Figure 4C, and it can be seen that the more the TA/Cu^{2+} nanoparticles, the more copper ions were released. It is worth noting that the hydrogels of each ratio can release copper ions slowly up to 1 week later, which indicates that the CMCS-TA/Cu^{2+} hydrogel has the effect of drug slow release. The probable reason is that CMCS and TA/Cu^{2+} nanoparticles can cross-link through a large number of hydrogen bonds to generate a strong force, which overcomes the disadvantage of the apparent sudden release, so that CMCS-TA/Cu^{2+} hydrogel can release stably for more than a week, allowing TA/Cu^{2+} nanoparticles to exert a sustained effect for a long period of time.

Cytocompatibility of Hydrogel Materials

Good biocompatibility is essential for materials that promote wound healing.[47] To establish the biocompatibility of the hydrogels, they have been co-cultured with HUVECs over 5 days and the presence of live cells has been detected using CCK-8 on days 1, 3, and 5. According to the OD450 results of the HUVECs cultured on the CMCS-TA/Cu^{2+} hydrogel (Figure 5A), the proliferative activity of the cells steadily increased as the culture time rose. The survival rate of HUVECs co-cultured on CMCS-TA/Cu^{2+} hydrogel exceeded 90% (Figure 5B). With prolonged incubation time, a significant increase in cell count on the hydrogel was observed after day 5 (Figure 5C). The cells adhered firmly and formed cell colonies gradually during the culture period. The overall findings suggest that the hydrogel exhibits favorable cytocompatibility.

Further observations of cell morphology (Figure 5D) verified that cells cultured on CMCS-TA/Cu^{2+} hydrogels exhibited a larger spreading area while maintaining an elongated spindle shape. In addition, greater cell adhesion and spreading of HUVECs was observed on CMCS-TA/Cu^{2+}-20%. According to the findings, CMCS-TA/Cu^{2+}-20% can more accurately replicate the in vivo tissue environment, which promotes cell development and enhances the effectiveness of tissue repair materials.

Cell Migration and Angiogenesis Analysis

The cell migration capability of the hydrogels was evaluated by examining the migration of HUVECs in vitro, as shown in Figure 6. Results from the experimentation in Figure 6A indicate that in terms of cell migration, with the increase in nanoparticle content, the cell migration rate was faster. In particular, the mobility of cells in CMCS-TA/Cu^{2+}-20% group reached 70% and 92% after 24 h and 48 h, respectively, which was significantly higher than that in other groups (Figure 6C). Furthermore, an appraisal was conducted on the impact of hydrogel on angiogenesis in HUVECs. Based on the analysis of the images and data demonstrated in Figure 6B – D, the CMCS-TA/Cu^{2+}-20% group manifested the highest lengths of blood vessels and the greatest number of tubes, which differed significantly from other hydrogel groups and showed a more pronounced effect in promoting angiogenesis. Copper ions can regulate the composition of extracellular matrix and the activity of enzymes, thus affecting the ability of cell adhesion, migration, and invasion. In addition, copper ions facilitate blood vessel formation by regulating the expression of vascular endothelial growth factors (such as VEGF) and matrix metalloproteinases (MMPs).[48] In TA/Cu^{2+} nanoparticles, Cu^{2+} is known to be strongly chelated with tannic acid resulting in limited release. However, the CMCS-TA/Cu^{2+}-20% hydrogel was found to release a higher amount of Cu^{2+} compared to other groups (albeit at a concentration that is not cytotoxic), resulting in a better effect on promoting cell migration and angiogenesis.

Wound Closure and Healing

As shown in Figure 7A, hydrogel can effectively seal the wound, resist bacterial invasion, and continuously release copper ions to promote wound healing. According to Figure 7B, the wounds in the two hydrogel groups showed a faster healing rate compared to the blank control group. After 9 days in the wound, there was no obvious scarring in the CMCS-TA/Cu^{2+} hydrogel composite group, whereas there was obvious scarring in both the CMCS hydrogel group as well as the control group. The CMCS-TA/Cu^{2+} exhibited a wound healing rate of 94.6%, while the CMCS group had a rate of 90.5% and the control group had 77.6% (Figure 7C). Following this, histology was performed to further discuss the healing of the skin wound. According to the photographs in Figure 6B and observation of H&E-stained tissue (Figure 7D), it is evident that the control group had a larger area of skin trauma than either the CMCS hydrogel group or the CMCS-TA/Cu^{2+} hydrogel composite group

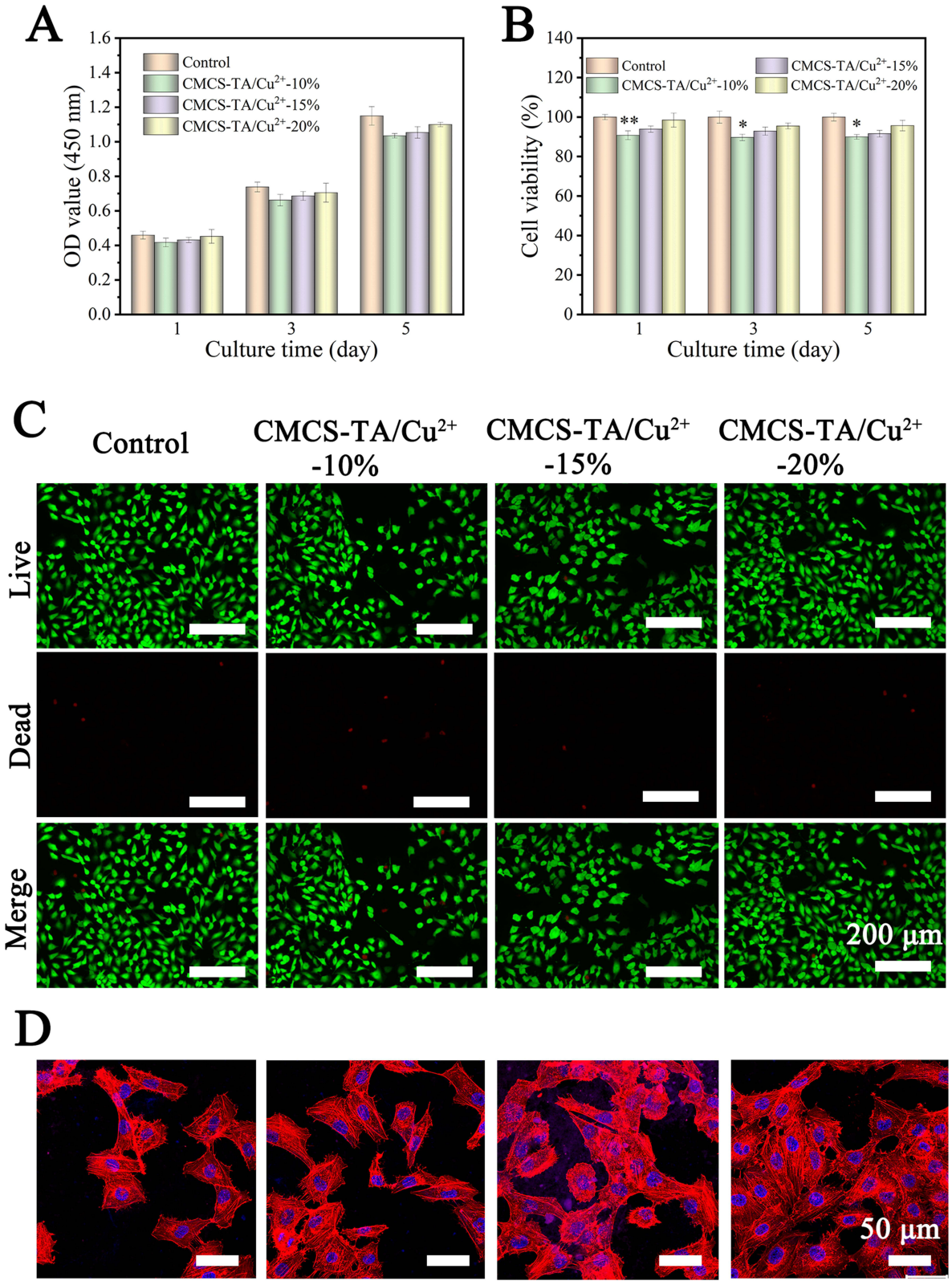

Figure 5 Results of in vitro cytocompatibility testing. (**A**) CCK-8 assay and (**B**) cell viability on hydrogels after 1, 3 and 5 days of culture. (**C**) Images of live/dead staining of cells following incubation on hydrogels. (**D**) Images taken using a confocal laser scanning microscope (CLSM) show HUVECs stained with rhodamine-coupled phalloidin (red) and DAPI (blue) after three days of growth. A one-way ANOVA was used to determine statistical significance: *$p < 0.05$, **$p < 0.01$.

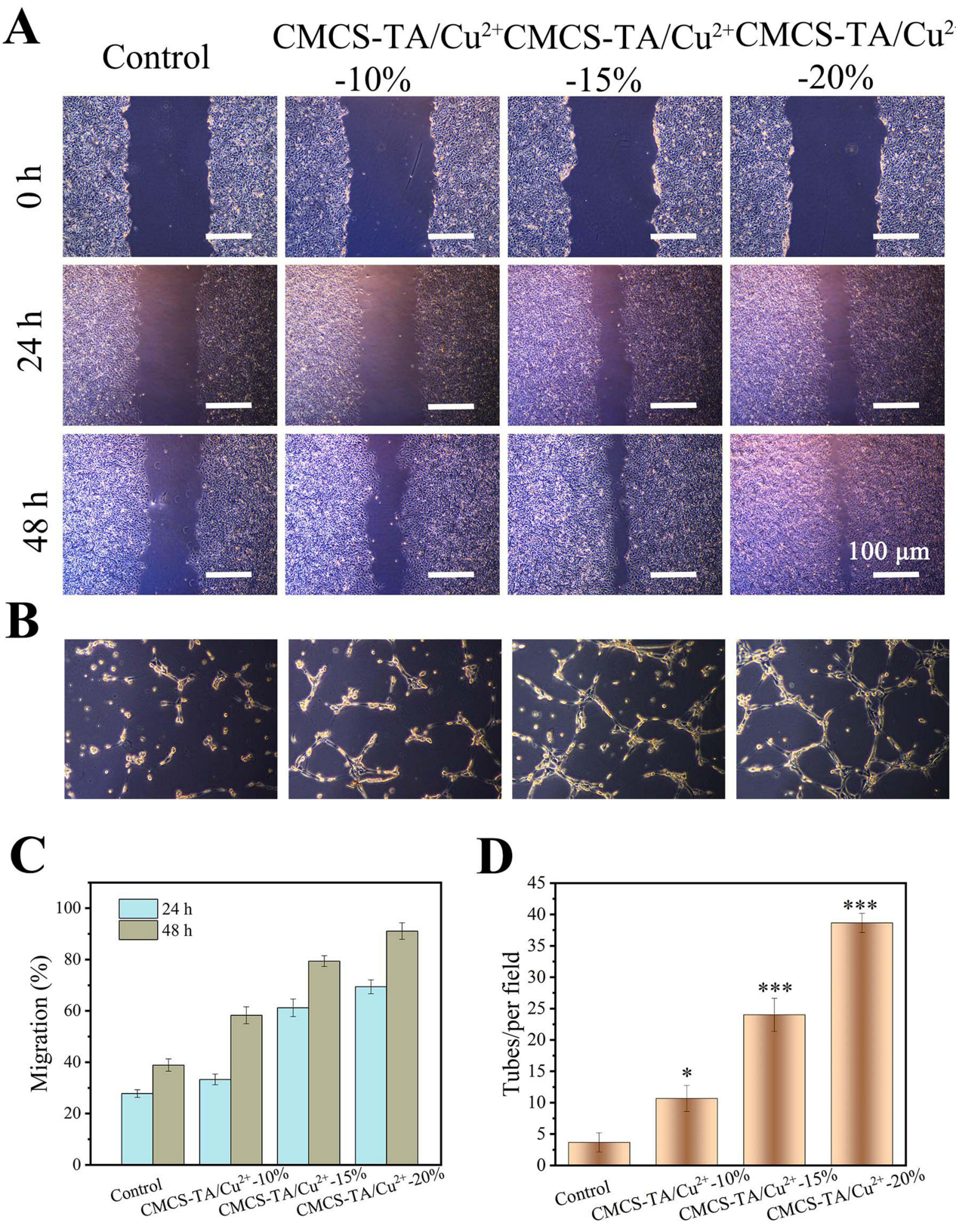

Figure 6 (**A**) Photographs of HUVECs migration. (**B**) Images of HUVECs tube formation in vitro. (**C**) Migration rate of HUVECs. (**D**) Statistical results of HUVECs tubes formation in co-culture with various hydrogels. A one-way ANOVA was used to determine statistical significance: *$p < 0.05$, ***$p < 0.001$.

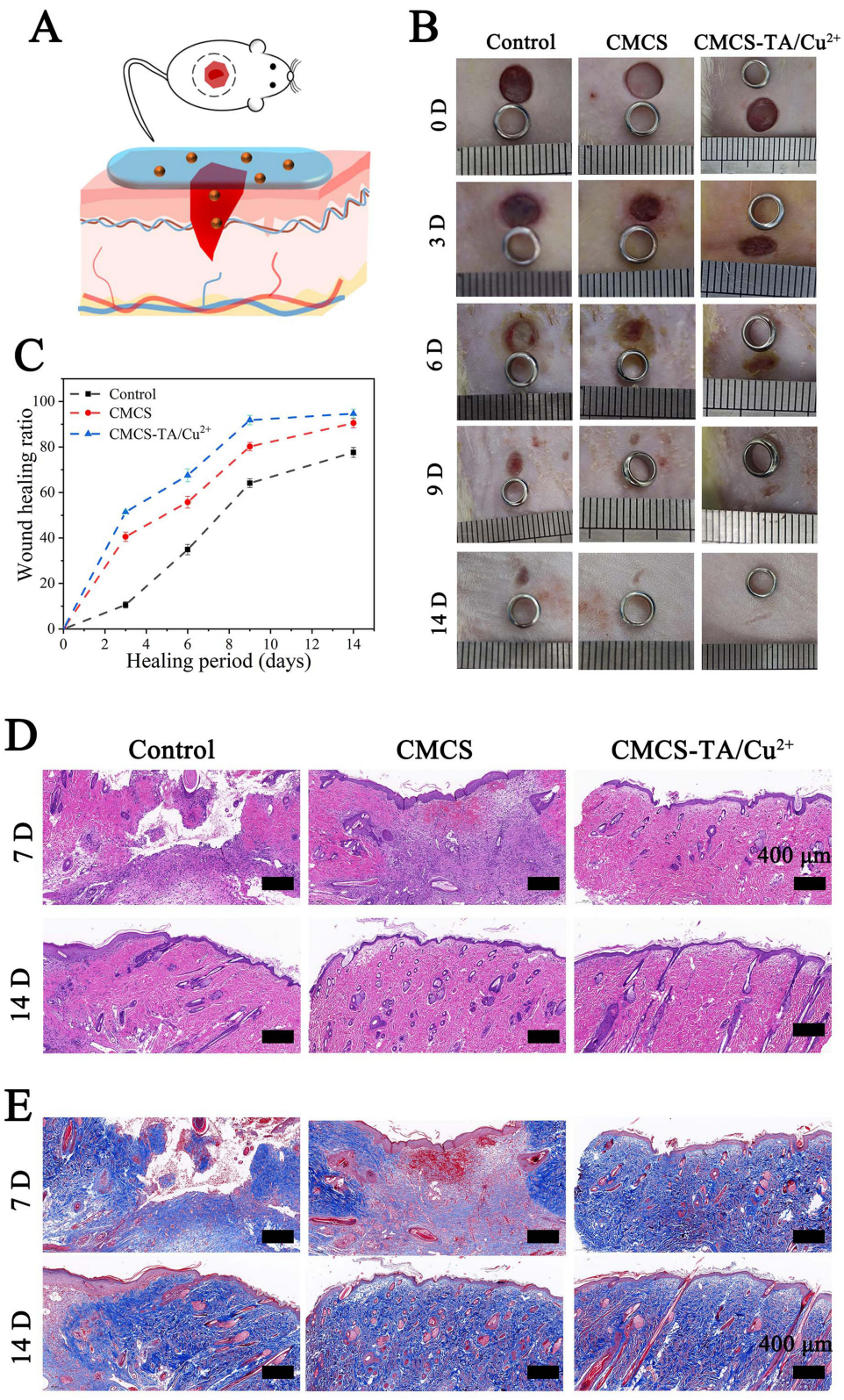

Figure 7 (**A**) Rat wound model. (**B**) Images showing the state of the wound at various times. (**C**) Wound healing rate. (**D**) H&E and (**E**) Masson staining on day 7 and 14 for various groups.

after 7 days of recovery. Inflammatory cell infiltration, migration, and fibroblast proliferation were seen in the sections of the CMCS hydrogel group, despite the fact that the group's outward appearance showed that the wounds had healed successfully. This indicated that an inflammatory response had taken place. Regarding the CMCS-TA/Cu^{2+} hydrogel group, the findings indicated successful healing, smooth and clean skin wound, complete regeneration of the epidermal layer, and glandular cavity regeneration in the dermis.

With the Control and CMCS hydrogel groups, the majority of the wounds had healed and were covered with fine hair after 14 days of wound healing. The control group showed persistent disorder in tissue arrangement, as revealed by H&E staining. The peri-wound tissue of the CMCS hydrogel group was neatly aligned, but there was no obvious regeneration of the dermal gland lumen. In the CMCS-TA/Cu^{2+} hydrogel group, not only was the peri-wound tissue well aligned but there was also obvious regeneration of the dermal gland lumen. Masson staining (Figure 7E) indicated an increase in collagen accumulation across all groups. The control group's collagen accumulation was relatively sparse, whereas the hydrogel group exhibited tightly arranged and orderly collagen accumulation, providing clear evidence of dermal glandular cavity regeneration in the CMCS-TA/Cu^{2+} hydrogel group. The histological analysis findings were indicative of the wound healing process being consistent. This suggests that the CMCS-TA/Cu^{2+} hydrogel proves effective in terms of wound closure and promotion of wound healing.

Conclusions

In this study, a CMCS-TA/Cu^{2+} composite hydrogel was developed by the low-temperature freeze-drying method and verified its potential in skin repair. The introduction of TA/Cu^{2+} nanoparticles not only enhanced the mechanical strength of the hydrogel, enriched the void structure of the hydrogel, but also continuously released copper ions, making the CMCS-TA/Cu^{2+} hydrogel has excellent antioxidant properties and promotes the ability of rapid wound repair. Carboxymethyl chitosan-based CMCS-TA/Cu^{2+} hydrogels also show excellent cytocompatibility. In co-culture with hydrogel experiments, the HUVECs could achieve rapid proliferation and show a good shape. More importantly, compared with blank group and CMCS hydrogel group, the CMCS-TA/Cu^{2+} hydrogel could better promote wound closure and healing with excellent healing effects and left no visible scars. Histological analysis shows that the hydrogel contributed to the formation of neatly aligned tissue structures and promoted collagen accumulation and regeneration of dermal glandular cavities. In summary, CMCS-TA/Cu^{2+} composite hydrogel has good free radical scavenging ability, cell compatibility, and promoting wound repair ability, which is a promising wound repair material.

Funding

This work was supported by National Natural Science Foundation of China (No.32300962), Natural Science Foundation of Guangdong Province (No.2021A1515111158), and Medical Scientific Research Foundation of Guangdong Province (No.C2022020).

Disclosure

The authors declare that they have no potential conflicts of interest regarding the research, authorship, and/or publication of this article.

References

1. Hosseini M, Shafiee A. Engineering bioactive scaffolds for skin regeneration. *Small*. 2021;17(41):e2101384. doi:10.1002/smll.202101384
2. Takeo M, Lee W, Ito M. Wound healing and skin regeneration. *Cold Spring Harb Perspect Med*. 2015;5(1):a023267. doi:10.1101/cshperspect.a023267
3. Chouhan D, Dey N, Bhardwaj N, et al. Emerging and innovative approaches for wound healing and skin regeneration: current status and advances. *Biomaterials*. 2019;216:119267.
4. Fiakos G, Kuang Z, Lo E. Improved skin regeneration with acellular fish skin grafts. *Eng Regen*. 2020;1:95–101. doi:10.1016/j.engreg.2020.09.002
5. Sun A, He X, Li L, et al. An injectable photopolymerized hydrogel with antimicrobial and biocompatible properties for infected skin regeneration. *NPG Asia Materials*. 2020;12(1): doi:10.1038/s41427-020-0206-y.
6. Zhang Q, Chang C, Qian C, et al. Photo-crosslinkable amniotic membrane hydrogel for skin defect healing. *Acta Biomater*. 2021;125:197–207. doi:10.1016/j.actbio.2021.02.043
7. Rahmati M, J BJ, P LS, et al. Designing multigradient biomaterials for skin regeneration. *Mater Today Adv*. 2020;5:100051.
8. Sahu A, Jeon J, S LM, et al. Antioxidant and anti-inflammatory activities of Prussian blue nanozyme promotes full-thickness skin wound healing. *Mater Sci Eng*. 2021;119:1.

9. Dong Y, Cui M, Qu J, et al. Conformable hyaluronic acid hydrogel delivers adipose-derived stem cells and promotes regeneration of burn injury. *Acta Biomater*. 2020;108:56–66. doi:10.1016/j.actbio.2020.03.040
10. M TE, Dorati R, Genta I, et al. Skin wound healing process and new emerging technologies for skin wound care and regeneration. *Pharmaceutics*. 2020;12:8.
11. Zhu Y, Ma Z, Kong L, et al. Modulation of macrophages by bioactive glass/sodium alginate hydrogel is crucial in skin regeneration enhancement. *Biomaterials*. 2020;256:120216. doi:10.1016/j.biomaterials.2020.120216
12. Zhang B, He J, Shi M, et al. Injectable self-healing supramolecular hydrogels with conductivity and photo-thermal antibacterial activity to enhance complete skin regeneration. *Chem Eng J*. 2020;400:1
13. Smandri A, Nordin A, M HN, et al. Natural 3D-printed bioinks for skin regeneration and wound healing: a systematic review. *Polymers*. 2020;12 (8):8. doi:10.3390/polym12081782
14. Geahchan S, Baharlouei P, Rahman A. Marine collagen: a promising biomaterial for wound healing, skin anti-aging, and bone regeneration. *Mar Drugs*. 2022;20(1):1. doi:10.3390/md20010061
15. Zhao D, Yu Z, Li Y, et al. GelMA combined with sustained release of HUVECs derived exosomes for promoting cutaneous wound healing and facilitating skin regeneration. *J Mol Histol*. 2020;51(3):251–263. doi:10.1007/s10735-020-09877-6
16. Chen L, Cheng L, Wang Z, et al. Conditioned medium-electrospun fiber biomaterials for skin regeneration. *Bioact Mater*. 2021;6(2):361–374. doi:10.1016/j.bioactmat.2020.08.022
17. Fathi A, Khanmohammadi M, Goodarzi A, et al. Fabrication of chitosan-polyvinyl alcohol and silk electrospun fiber seeded with differentiated keratinocyte for skin tissue regeneration in animal wound model. *J Biol Eng*. 2020;14(1):27. doi:10.1186/s13036-020-00249-y
18. Li S, Dong Q, Peng X, et al. Self-healing hyaluronic acid nanocomposite hydrogels with platelet-rich plasma impregnated for skin regeneration. *ACS Nano*. 2022;16(7):11346–11359. doi:10.1021/acsnano.2c05069
19. Uppuluri V, Thukani Sathanantham S, K BS, et al. Polymeric hydrogel scaffolds: skin tissue engineering and regeneration. *Adv Pharm Bull*. 2022;12(3):437–448. doi:10.34172/apb.2022.069
20. Kalai Selvan N, Shanmugarajan TS, Uppuluri VNV. A Hydrogel based scaffolding polymeric biomaterials: approaches towards skin tissue regeneration. *J Drug Delivery Sci Technol*. 2020;55:1.
21. Dussoyer M, Michopoulou A, Rousselle P. Decellularized scaffolds for skin repair and regeneration. *Appl Sci*. 2020;10(10):10. doi:10.3390/app10103435
22. Morgun EI, Vorotelyak E. A epidermal stem cells in hair follicle cycling and skin regeneration: a view from the perspective of inflammation. *Front Cell Dev Biol*. 2020;8:581697. doi:10.3389/fcell.2020.581697
23. Guo B, Liang Y, Dong R, P JN. Physical dynamic double-network hydrogels as dressings to facilitate tissue repair. *Mater Today Adv*. 2023;2023: 1–33.
24. Liang Y, Li Z, Huang Y, et al. Dual-dynamic-bond cross-linked antibacterial adhesive hydrogel sealants with on-demand removability for post-wound-closure and infected wound healing. *ACS nano*. 2021;15(4):7078–7093. doi:10.1021/acsnano.1c00204
25. Cao J, Wu P, Cheng Q, et al. Ultrafast fabrication of self-healing and injectable carboxymethyl chitosan hydrogel dressing for wound healing. *ACS Appl Mater Interfaces*. 2021;13(20):24095–24105. doi:10.1021/acsami.1c02089
26. Feng X, Hou X, Cui C, et al. Mechanical and antibacterial properties of tannic acid-encapsulated carboxymethyl chitosan/polyvinyl alcohol hydrogels. *Eng Regen*. 2021;2:57–62. doi:10.1016/j.engreg.2021.05.002
27. Yu N, Li Y, Wang Y, et al. Healing effect of carboxymethyl chitosan-plantamajoside hydrogel on burn wound skin. *Burns*. 2022;48(4):902–914. doi:10.1016/j.burns.2022.01.019
28. Qianqian O, Songzhi K, Yongmei H, et al. Preparation of nano-hydroxyapatite/chitosan/tilapia skin peptides hydrogels and its burn wound treatment. *Int J Biol Macromol*. 2021;181:369–377.
29. G FP, F FV, da Silva FC, et al. Chitosans and nanochitosans: recent advances in skin protection, regeneration, and repair. *Pharmaceutics*. 2022;14:6.
30. Keirouz A, Zakharova M, Kwon J, et al. High-throughput production of silk fibroin-based electrospun fibers as biomaterial for skin tissue engineering applications. *Mater Sci Eng C*. 2020;112:1
31. Guo F, Liu Y, Chen S, et al. A Schiff base hydrogel dressing loading extracts from Periplaneta Americana for diabetic wound healing. *Int J Biol Macromol*. 2023;230:123256.
32. L GB, Han P, C GL, et al. The antibacterial activity of ta-doped ZnO nanoparticles. *Nanoscale Res Lett*. 2015;10(1):1047. doi:10.1186/s11671-015-1047-4
33. He M, Wang Z, Yang H, et al. multi-functional bio-hjzyme: revolutionizing diabetic skin regeneration with its glucose-unlocked sterilization and programmed anti-inflammatory effects. *Adv Sci*. 2023;10(21):e2300986. doi:10.1002/advs.202300986
34. Feng H, Zhang J, Yang W, et al. Transparent janus hydrogel wet adhesive for underwater self-cleaning. *ACS Appl Mater Interfaces*. 2021;13 (42):50505–50515. doi:10.1021/acsami.1c12696
35. Xiao Y, Peng J, Liu Q, et al. Ultrasmall CuS@BSA nanoparticles with mild photothermal conversion synergistically induce MSCs-differentiated fibroblast and improve skin regeneration. *Theranostics*. 2020;10(4):1500–1513. doi:10.7150/thno.39471
36. Li Q, Song H, Li S, et al. Macrophage metabolism reprogramming EGCG-Cu coordination capsules delivered in polyzwitterionic hydrogel for burn wound healing and regeneration. *Bioactive Materials*. 2023;29:251–264. doi:10.1016/j.bioactmat.2023.07.011
37. Zhao J, Liu Y, Pan B, et al. Tannic acid promotes ion release of copper oxide nanoparticles: impacts from solution pH change and complexation reactions. *Water Res*. 2017;127:59–67. doi:10.1016/j.watres.2017.10.006
38. Lin S, Cheng Y, Zhang H, et al. Copper tannic acid coordination nanosheet: a potent nanozyme for scavenging ROS from cigarette smoke. *Small*. 2020;16(27):1902123.
39. Huang L, Zhu Z, Wu D, et al. Antibacterial poly (ethylene glycol) diacrylate/chitosan hydrogels enhance mechanical adhesiveness and promote skin regeneration. *Carbohydr Polym*. 2019;225:115110. doi:10.1016/j.carbpol.2019.115110
40. Liu H, Hu X, Li W, et al. A highly-stretchable and adhesive hydrogel for noninvasive joint wound closure driven by hydrogen bonds. *Chem Eng J*. 2023;452:139368
41. Liu G, Bao Z, Wu J. Injectable baicalin/F127 hydrogel with antioxidant activity for enhanced wound healing. *Chin Chem Lett*. 2020;31 (7):1817–1821. doi:10.1016/j.cclet.2020.03.005
42. Rinkevich Y JD. Scars or regeneration?-Dermal fibroblasts as drivers of diverse skin wound responses. *Int J Mol Sci*. 2020;21:2.

43. Huang L, Li W, Guo M, et al. Silver doped-silica nanoparticles reinforced poly (ethylene glycol) diacrylate/hyaluronic acid hydrogel dressings for synergistically accelerating bacterial-infected wound healing. *Carbohydr Polym*. 2023;304:120450. doi:10.1016/j.carbpol.2022.120450
44. Wier EM, Garza L. A through the lens of hair follicle neogenesis, a new focus on mechanisms of skin regeneration after wounding. *Semin Cell Dev Biol*. 2020;100:122–129. doi:10.1016/j.semcdb.2019.10.002
45. Wang C-H, Hsieh D-J, Periasamy S, et al. Regenerative porcine dermal collagen matrix developed by supercritical carbon dioxide extraction technology: role in accelerated wound healing. *Materialia*. 2020;9:100576. doi:10.1016/j.mtla.2019.100576
46. Fu Y, Zhang J, Wang Y, et al. Reduced polydopamine nanoparticles incorporated oxidized dextran/chitosan hybrid hydrogels with enhanced antioxidative and antibacterial properties for accelerated wound healing. *Carbohydrate Polymers*. 2021;257:117598. doi:10.1016/j.carbpol.2020.117598
47. Chen J, He J, Yang Y, et al. Antibacterial adhesive self-healing hydrogels to promote diabetic wound healing. *Acta biomaterialia*. 2022;146:119–130. doi:10.1016/j.actbio.2022.04.041
48. Huang W, Xu P, Fu X, et al. Functional molecule-mediated assembled copper nanozymes for diabetic wound healing. *Journal of Nanobiotechnology*. 2023;21(1):294. doi:10.1186/s12951-023-02048-1